Quantum-chromodynamic predictions for direct photons in e^+e^- collisions. II. Analysis of the third and fourth structure functions $\overline{W}_3^\gamma$ and $\overline{W}_4^\gamma$

Ken Sasaki

Fermi National Accelerator Laboratory, Batavia, Illinois 60510
and Department of Physics, Faculty of Education, Yokohama National University, Yokohama 240, Japan†

We analyze in quantum chromodynamics the timelike photon structure functions $\overline{W}_3^\gamma$ and $\overline{W}_4^\gamma$ which appear in the direct photon production in e^+e^- collisions, using the cut-vertex formalism and the renormalization-group method. It is found that $\overline{W}_3^\gamma$ in leading order is not renormalized by the strong interactions and agrees with the result calculated in the simple parton model. The moments of $\overline{W}_4^\gamma$ are calculated in the leading order. Then, the structure function is obtained by inverting the moments. The corrections to $\overline{W}_4^\gamma$ by strong interactions are found to be large at small and large z.

I. INTRODUCTION

At very high energies in e^+e^- colliding experiments the direct photon production in such processes as shown in Fig. 1,

$$e^+e^- \rightarrow \gamma^*(q) \rightarrow \gamma_{\text{direct}}(p) + \text{hadrons}(C=+) , \tag{1.1}$$

becomes measurable. Here the virtual photon with momentum q is far off shell (large $q^2 > 0$) and the observed photon having momentum p is "direct, " which means that it is not a decay product of radiatively decaying hadrons. The unobserved hadrons have charge conjugation $C=+$.

From the above experiments of Eq. (1.1), we can measure the timelike photon structure functions, which are defined as[1]

$$\overline{W}^{\mu\nu\rho\tau} = \frac{1}{2\pi} \int \int \int d^4x\, d^4y\, d^4z\, e^{iq\cdot z}e^{ip\cdot(y-x)} \langle 0 | \overline{T}(J^\rho(x)J^\mu(z))T(J^\tau(y)J^\nu(0)) | 0 \rangle$$

$$= \left[-g^{\mu\nu}+\frac{q^\mu q^\nu}{q^2} \right]\left[-g^{\rho\tau}+\frac{q^\rho p^\tau+p^\rho q^\tau}{p\cdot q} \right]\overline{W}_1^\gamma + \left[p^\mu-\frac{p\cdot q}{q^2}q^\mu \right]\left[p^\nu-\frac{p\cdot q}{q^2}q^\nu \right]\left[-g^{\rho\tau}+\frac{q^\rho p^\tau+p^\rho q^\tau}{p\cdot q} \right]\overline{W}_2^\gamma$$

$$+ \left[\left[-g^{\mu\rho}+\frac{p^\mu q^\rho}{p\cdot q} \right]\left[-g^{\nu\tau}+\frac{p^\nu q^\tau}{p\cdot q} \right]+\left[-g^{\mu\tau}+\frac{p^\mu q^\tau}{p\cdot q} \right]\left[-g^{\nu\rho}+\frac{p^\nu q^\rho}{p\cdot q} \right] \right]$$

$$- \left[-g^{\mu\nu}+\frac{p^\mu q^\nu+q^\mu p^\nu}{p\cdot q}-\frac{p^\mu p^\nu q^2}{(p\cdot q)^2} \right]\left[-g^{\rho\tau}+\frac{q^\rho p^\tau+p^\rho q^\tau}{p\cdot q} \right]\overline{W}_3^\gamma$$

$$+ \left[\left[-g^{\mu\rho}+\frac{p^\mu q^\rho}{p\cdot q} \right]\left[-g^{\nu\tau}+\frac{p^\nu q^\tau}{p\cdot q} \right]-\left[-g^{\mu\tau}+\frac{p^\mu q^\tau}{p\cdot q} \right]\left[-g^{\nu\rho}+\frac{p^\nu q^\rho}{p\cdot q} \right] \right]\overline{W}_4^\gamma , \tag{1.2}$$

where $\overline{T}$ represents anti-time-ordered products.

In a previous paper,[2] we have analyzed the structure functions $\overline{W}_T^\gamma\ (=\overline{W}_1^\gamma)$ and $\overline{W}_L^\gamma$ $(=\overline{W}_1^\gamma+[(p\cdot q)^2/q^2]\overline{W}_2^\gamma)$ in quantum chromodynamics (QCD). Using the cut-vertex formalism[3] and renormalization-group method we have calculated the moments of $\overline{W}_T^\gamma$ up to the next-to-leading order, and the moments of $\overline{W}_L^\gamma$ in the leading order.

In this paper we shall analyze the structure functions $\overline{W}_3^\gamma$ and $\overline{W}_4^\gamma$ in QCD with f flavors.

The information on $\overline{W}_3^\gamma$ can be extracted from experiments with unpolarized e^+e^- beams, where the linear polarization of the final photon is mea-
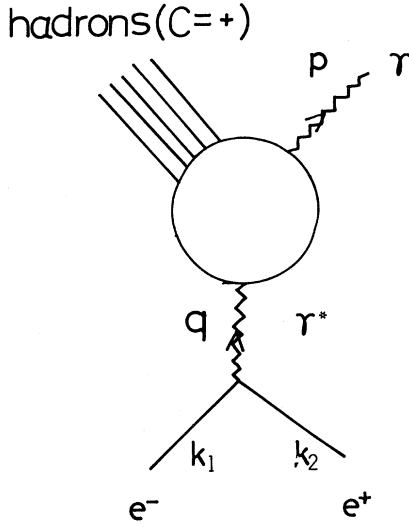
FIG. 1. Direct production of photons in e^+e^- collisions. The observed photons are assumed not to be radiative decay products of hadrons.

sured with respect to the plane spanned by the electron (or positron) and photon momentum.[1] The structure function $\overline{W}_4^\gamma$ can be obtained by observing circularly polarized final photons from annihilations of polarized electrons (positrons) and unpolarized positrons (electrons). In the Appendix, we express differential cross sections of

$$e^+e^- \rightarrow \gamma^* \rightarrow \gamma_{\text{direct}} + \text{hadrons}(C=+)$$

in terms of photon structure functions for the cases of unpolarized- and polarized-beam experiments.

In the free-quark model, i.e., the parton model (PM), the structure functions $\overline{W}_3^\gamma$ and $\overline{W}_4^\gamma$ can be calculated by evaluating the s-channel discontinuity of the box diagrams of Fig. 2. We obtain

$$\overline{W}_3^\gamma \Big|_{\text{PM}} = \alpha^2 \delta_\gamma \left[-\frac{4}{z^2} \right] \tag{1.3}$$

and

$$\overline{W}_4^\gamma \Big|_{\text{PM}} = \alpha^2 \delta_\gamma 4 \frac{2-z}{z} \ln \frac{q^2(1-z)}{m_q^2} , \tag{1.4}$$

where $\alpha = e^2/4\pi$, $z = 2p \cdot q/q^2$, m_q is the quark mass, and

$$\delta_\gamma = 3f\langle e^4 \rangle = 3\sum_i e_i^4 , \tag{1.5}$$

the sum i runs over quarks of f flavors. Because of the pointlike coupling of photon to quarks $\overline{W}_4^\gamma \big|_{\text{PM}}$ does not scale, but grows logarithmically
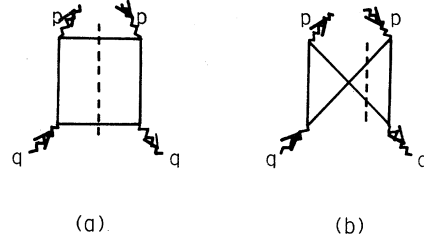

FIG. 2. Box diagrams for direct photon production.

with q^2. On the other hand, $\overline{W}_3^\gamma \big|_{\text{PM}}$ displays Bjorken scaling.

We now study the behaviors of the structure functions $\overline{W}_3^\gamma$ and $\overline{W}_4^\gamma$ in QCD using Mueller's cut-vertex formalism[3,4] and the renormalization-group techniques. The cut-vertex method is powerful when it is applied to such processes as single-particle production in e^+e^- collisions where the operator-product expansion is not applicable. By this method the moments of the structure functions in single-particle inclusive e^+e^- annihilation can be written in a factorized form for large q^2; a coefficient function depending on the q^2 of the virtual photon, but completely independent of the particle produced, times a cut vertex which depends on the particle observed. The q^2 dependence of the coefficient functions is governed by the renormalization-group equation (RGE). Then, solving the RGE, we can evaluate in QCD the moments of the structure functions systematically order by order in perturbation.

We analyze the photon structure functions $\overline{W}_3^\gamma$ and $\overline{W}_4^\gamma$ in the leading order. We find that $\overline{W}_4^\gamma$ maintains the nonscaling $\ln q^2$ behavior, but its shape changes substantially from the simple parton-model prediction. However, $\overline{W}_3^\gamma$ in the leading order is found not to be renormalized by the strong interactions and to have the same expression as obtained in the parton model. The results are very similar to the case of deep-inelastic scattering off a photon target ($q^2 < 0$ in this case) where the spacelike photon structure function W_4^γ shows a different nonscaling $\ln(-q^2)$ behavior from the PM prediction, but W_3^γ in the leading order is not affected by strong-interaction effects and agrees with the result calculated in the parton model.[5-7]

In Sec. II we analyze the structure function $\overline{W}_4^\gamma$. We introduce *new* bare cut vertices for fermions, gluons, and photons which contribute to $\overline{W}_4^\gamma$. (These fermion and gluon cut vertices are also applicable to the study of polarized nucleon production in collisions of polarized e^+e^- beams.) Then,
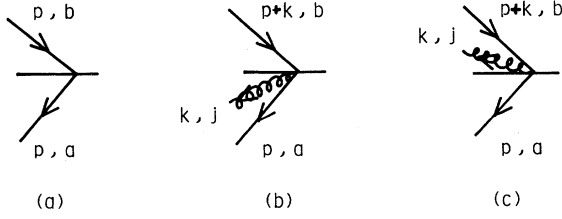
FIG. 3. The cut vertices for two fermions contributing to $\overline{W}_4^\gamma$. (a) $R_{\psi,n}^{ab}(p)$. (b) $R_{\psi,n}^{aj,b}(p,k)$. (c) $R_{\psi,n}^{a,bj}(p,k)$. Solid lines and curly lines represent quarks and gluons, respectively.

we calculate the one-loop anomalous dimensions of the relevant cut vertices. Using these anomalous dimensions we obtain the QCD prediction for the leading term of $\overline{W}_4^\gamma$ moments. The structure function $\overline{W}_4^\gamma$ itself is obtained by inverting the moments numerically. In Sec. III we analyze $\overline{W}_3^\gamma$. We discuss in some detail why bare cut vertices for fermions do not contribute to $\overline{W}_3^\gamma$ in the leading order. Section IV is devoted to a brief summary.

II. STRUCTURE FUNCTION $\overline{W}_4^\gamma$

First we must find the projection operator which picks up the structure function $\overline{W}_4^\gamma$ from $\overline{W}_{\mu\nu\rho\tau}$ in Eq. (1.2). The appropriate operator is $\frac{1}{4}\epsilon_{-+\mu\nu}\epsilon_{-+\rho\tau}$, and we obtain

$$\frac{1}{4}\epsilon_{-+\mu\nu}\epsilon_{-+\rho\tau}\overline{W}^{\mu\nu\rho\tau} \approx \overline{W}_4^\gamma , \qquad (2.1)$$

where q_- and p_μ are finite with large q^2 and q_+.[8]

Using Mueller's cut-vertex formalism, we now show the moments of $\overline{W}_4^\gamma$ can be written in a factorized form, i.e., the sum of terms each of which is a product of a cut vertex and a timelike coefficient function.

A. Cut vertices for $\overline{W}_4^\gamma$

We need to introduce new cut vertices for the analysis of $\overline{W}_4^\gamma$. We list, in the following, necessary (timelike) cut vertices. Those vertices for fermions and gluons will also be applicable to the analysis of the polarized nucleon production in polarized e^+e^- collisions.

The flavor-singlet cut vertices for two fermions without and with one gluon are

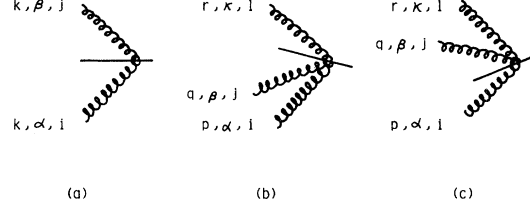Fig. 3(a): $R_{\psi,n}^{ab}(p) = i\gamma_-\gamma_5 p_-^{-n-2}\delta_{ab}\mathbf{1}$,

FIG. 4. The cut vertices for gluons contributing to $\overline{W}_4^\gamma$. (a) $R_{\alpha\beta,n}^{ij}(k)$. (b) $R_{\alpha\beta,\kappa;n}^{ij,l}(p,q,r)$. (c) $R_{\alpha,\beta\kappa;n}^{i,jl}(p,q,r)$.

Fig. 3(b): $R_{\psi,n}^{aj,b}(p,k) = ig\dfrac{\gamma_-\gamma_5}{k_-}$

$$\times T_{ab}^j(p+k)_-^{-n-2}\mathbf{1} ,$$

$$(2.2)$$

Fig. 3(c): $R_{\psi,n}^{a,bj}(p,k) = -ig\dfrac{\gamma_-\gamma_5}{k_-}T_{ab}^j p_-^{-n-2}\mathbf{1} .$$

The indices a,b refer to a representation R of the color group SU(3) for fermions, g is the strong coupling constant of the theory, and $\mathbf{1}$ is the $f \times f$ unit matrix. These vertices obey the following Ward-Takahashi (WT) identities:

$$k_-R_{\psi,n}^{ai,b}(p,k) = gT_{aa'}^iR_{\psi,n}^{a'b}(p+k) ,$$

$$k_-R_{\psi,n}^{a,bi}(p,k) = -gR_{\psi,n}^{ab'}(p)T_{b'b}^i . \qquad (2.3)$$

We must add the cut vertices for two fermions with more gluons. Vertices with extra gluons become rather complicated, but their form is essentially fixed by the WT identities and the bare fermion cut vertices without gluons. Therefore we have not listed higher-order vertices.

The formula for the flavor-nonsinglet cut vertices for two fermions without and with gluons are the same as the singlet ones with the replacement of $\mathbf{1}$ by $(Q_{ch}^2 - \langle e^2\rangle\mathbf{1})$, where Q_{ch}^2 is the square of the $f \times f$ quark charge matrix, and $\langle e^2 \rangle$ is the average quark charge squared.

The cut vertex for two gluons shown in Fig. 4(a) is

$$R_{\alpha\beta,n}^{ij}(k) = 2\delta_{ij}[(g_{1\alpha}g_{2\beta}k_-^2 - g_{-\alpha}g_{2\beta}k_1k_-$$

$$-g_{1\alpha}g_{-\beta}k_2k_- - (\alpha\leftrightarrow\beta)]k_-^{-n-3} . \qquad (2.4)$$

We need cut vertices for more gluons. The three-gluon vertices are shown in Figs. 4(b) and 4(c). They are given by

$$R^{ij,l}_{\alpha\beta,\kappa;n}(p,q,r)=2ig\left\{\frac{C_{ijl}g_{-\beta}}{q_-}\{[(g_{1\kappa}g_{2\alpha}p_- -g_{-\kappa}g_{2\alpha}p_1 -g_{1\kappa}g_{-\alpha}p_2)-(\alpha\leftrightarrow\kappa)]r_-\right.$$

$$-[(r_1g_{2\alpha}-g_{1\alpha}r_2)p_- -(r_-g_{2\alpha}-g_{-\alpha}r_2)p_1 -(r_1g_{-\alpha}-g_{1\alpha}r_-)p_2]g_{-\kappa}\}$$

$$+C_{ijl}\{[g_{1\kappa}g_{2\alpha}g_{-\beta}+g_{2\kappa}g_{-\alpha}g_{1\beta}-g_{-\kappa}g_{2\alpha}g_{1\beta}]r_-$$

$$-[r_1g_{2\alpha}g_{-\beta}+r_2g_{-\alpha}g_{1\beta}-r_-g_{2\alpha}g_{1\beta}]g_{-\kappa}\}$$

$$+ \text{ terms where }(i,\alpha,p)\leftrightarrow(j,\beta,q)\bigg\}r_-^{-n-3} , \qquad (2.5)$$

where C_{ijl} are the structure constants of the color group. $R^{i,jl}_{\alpha,\beta\kappa;n}(p,q,r)$ is obtained from $R^{ij,l}_{\alpha\beta,\kappa;n}(p,q,r)$ as follows. (i) Change r_-^{-n-3} to $-(-p_-)^{-n-3}$; (ii) interchange $(i,\alpha,p)\leftrightarrow(l,\kappa,r)$ in all terms in large curly brackets of Eq. (2.5).

These vertices satisfy the WT identities

$$q^{\beta}R^{ij,l}_{\alpha\beta,\kappa;n}(p,q,r)=igC_{ijm}R^{ml}_{\alpha\kappa,n}(r) ,$$

$$q^{\beta}R^{i,jl}_{\alpha,\beta\kappa;n}(p,q,r)=igC_{ljm}R^{mi}_{\alpha\kappa;n}(-p) , \qquad (2.6)$$

and the current-conservation law

$$r^{\kappa}R^{ij,l}_{\alpha\beta,\kappa;n}(p,q,r)=0 ,$$

$$p^{\alpha}R^{i,jl}_{\alpha,\beta\kappa;n}(p,q,r)=0 . \qquad (2.7)$$

Also note that $R^{ij,l}_{\alpha\beta,\kappa;n}(p,q,r)$ and $R^{i,jl}_{\alpha,\beta\kappa;n}(p,q,r)$ are symmetric under the interchange of indices $(i,\alpha,p)\leftrightarrow(j,\beta,q)$ and $(j,\beta,q)\leftrightarrow(l,\kappa,r)$, respectively. Cut vertices with more gluons are straightforward to construct with resort to the WT identities and the current conservation law.

Finally we introduce the bare cut vertex for two photons illustrated in Fig. 5:

$$R^{\gamma}_{\alpha\beta,n}(p)=2[(g_{1\alpha}g_{2\beta}p_-^2-g_{-\alpha}g_{2\beta}p_1p_-$$

$$-g_{1\alpha}g_{-\beta}p_2p_-)-(\alpha\leftrightarrow\beta)]p_-^{-n-3} . \qquad (2.8)$$

The expression of Eq. (2.8) is exactly the same form as the two-gluon cut vertex of Eq. (2.4) apart from the factor δ_{ij}.

It will be apparent in the following why these cut vertices have been introduced.

B. Factorization

We consider a particular graph G contributing to $\overline{W}^{\gamma}_4$. Suppose G can be decomposed topologically

as shown in Fig. 6 (a), where large momenta of order q^2 flow through the right-hand part τ, but not through the left-hand part λ. The two parts are connected by two quark propagators which are included in λ. For a while we neglect the color and flavor degrees of freedom of quarks. Call $M^{\tau}_{\mu\nu}(k,q)$ the renormalized right-hand part, and we may write

$$M^{\tau}_{\mu\nu}(k,q)=\sum_i t^i_{\mu\nu}(k,q)M^{\tau}_i(k^2,k\cdot q,q^2) , \qquad (2.9)$$

where the $t^i_{\mu\nu}$ are matrices in the Dirac indices and the M^{τ}_i are dimensionless. The rules to find the contributing $t^i_{\mu\nu}$ when $q^2\to\infty$ are as follows. (i) The tensors should be antisymmetric in μ and ν. Hence they have $\epsilon_{\mu\nu\alpha\beta}$ and γ_5. (ii) They are linear in γ aside from γ_5. (iii) Only conserved tensors need be considered, since slightly off-shell fermions will not inhibit current conservation when the momentum q flows through τ. (iv) Drop all terms with explicit factors of m^2 (quark mass squared) or k^2. (v) Drop all terms with k compared to q. The allowed tensors are
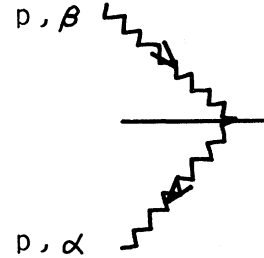

FIG. 5. The cut vertex for two photons contributing to $\overline{W}^{\gamma}_4$.

$$t^1_{\mu\nu}=i\epsilon_{\mu\nu\alpha\beta}\frac{q^\alpha\gamma^\beta}{q^2}\gamma_5 , \tag{2.10}$$

$$t^2_{\mu\nu}=i\epsilon_{\mu\nu\alpha\beta}\frac{q^\alpha k^\beta}{q^2}\frac{q\!\!\!/}{q^2}\gamma_5 . \tag{2.11}$$

Writing

$$\tfrac{1}{2}\epsilon_{-+}{}^{\mu\nu}M^\tau_{\mu\nu}(k,q)=M^\tau_{-+}(k,q) , \tag{2.12}$$

we obtain for large q_+ with finite q_- and k_μ,

$$M^\tau_{-+}(k,q)\approx iq_+\gamma_-\gamma_5\frac{1}{q^2}M^\tau(k^2,k\cdot q,q^2) , \tag{2.13}$$

where

$$M^\tau(k^2,k\cdot q,q^2)=M^\tau_1(k^2,k\cdot q,q^2)$$
$$+\frac{k_-}{2q_-}M^\tau_2(k^2,k\cdot q,q^2) . \tag{2.14}$$

Now we define the additional subtraction dictated t^τ for M^τ_{-+} as follows:

$$t^\tau M^\tau_{-+}(k,q)=iq_+\gamma_-\gamma_5\frac{1}{q^2}M^\tau(0,\hat{k}\cdot q,q^2) , \tag{2.15}$$

where $\hat{k}_+=\hat{k}_\perp=0$ and $\hat{k}_-=k_-$.

For the contribution of Fig. 6(a) to $\overline{W}^\gamma_4$, we can write

$$\tfrac{1}{4}\epsilon_{-+}{}^{\mu\nu}\epsilon_{-+}{}^{\rho\tau}\overline{W}_{\mu\nu\rho\tau}= \int \frac{d^4k}{(2\pi)^4}[\tfrac{1}{2}\epsilon_{-+}{}^{\rho\tau}T^\lambda_{\rho\tau}(p,k)]_{rs}[t^\tau M^\tau_{-+}(k,q)]_{rs} , \tag{2.16}$$

where

$$[T^\lambda_{\rho\tau}(p,k)]_{rs}=\frac{1}{2\pi} \int \int \int d^4x\, d^4y\, d^4z\, e^{ikz}e^{ip(y-x)} \langle 0| \overline{T}(J_\rho(x)\psi_r(z))T(J_\tau(y)\overline{\psi}_s(0))|0\rangle \tag{2.17}$$

and r,s are the Dirac indices. We neglect the renormalization of $T^\lambda_{\rho\tau}(p,k)$ for the moment. From Eqs. (2.1) and (2.15), Eq. (2.16) is rewritten as

$$\overline{W}^\gamma_4=\frac{q_+}{q^2} \int \frac{d^4k}{(2\pi)^4}[T^\lambda_{-+}(p,k)]_{rs}(i\gamma_-\gamma_5)_{rs}$$
$$\times M^\tau(0,\hat{k}\cdot q,q^2) \tag{2.18}$$

with

$$T^\lambda_{-+}(p,k)=\tfrac{1}{2}\epsilon_{-+}{}^{\rho\tau}T^\lambda_{\rho\tau}(p,k) . \tag{2.19}$$

We note the coupling of T^λ_{-+} to M^τ is only through k_-. Then, taking the moments of both sides of Eq. (2.18), we find

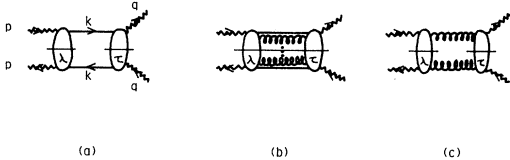$$\int_0^1 dz\, z^n\overline{W}_4=v_nE_{4,n}(q^2) , \tag{2.20}$$

(a)   (b)   (c)

FIG. 6. Examples of decompositon of the amplitude for direct photon production in e^+e^- annihilation: (a) involving two fermions; (b) involving two fermions and many gluons; (c) involving two gluons. Wavy lines represent photons.

where

$$v_n=\tfrac{1}{2}p_-{}^{-n+1} \int \frac{d^4k}{(2\pi)^4}[T^\lambda_{-+}(p,k)]_{rs}$$
$$\times(i\gamma_-\gamma_5)_{rs}k_-{}^{-n-2} \tag{2.21}$$

and

$$E_{4,n}(q^2)= \int_0^1 d\tilde{z}\,\tilde{z}^{n+1}M(1,\tilde{z},q^2) \tag{2.22}$$

with $\tilde{z}=2\hat{k}\cdot q/q^2$. Equation (2.20) shows that the moments of $\overline{W}^\gamma_4$ can be written in a factorized form. A bare cut vertex for two fermions [see Eq. (2.2)] is involved in v_n of Eq. (2.21). At this point v_n is the unrenormalized cut vertex. After renormalizing the cut vertex, we obtain an equation just like Eq. (2.20), except that v_n is now renormalized. The renormalization prescription for cut vertices is described in detail in Ref. 3.

Next we consider a decomposition of the form shown in Fig. 6(b), where two fermions and an arbitrary number of gluons connect the two parts of the graph. Suppose

$$M^\tau_{\alpha_1\cdots\alpha_j,\mu\nu}(k_1,\cdots,k_j,k,q)$$

is the renormalized amplitude for the right-hand part τ. $\alpha_1,\cdots,\alpha_j$ are the Lorentz indices of gluons and the divergent part, for large q^2, has all $+$ indices. Owing to the WT identity,

$$\prod_{i=1}^{j} k_{i-} M_{+\,\cdots\,+,\mu\nu}^{\tau}(k_1,\cdots,k_j,k,q) \qquad (2.23)$$

is expressed in terms of the amplitudes $M_{+\,\cdots\,+,\mu\nu}$ with two fermions, but *fewer gluons*. Thus by repeated use of the WT identities, $M_{+\,\cdots\,+,\mu\nu}^{\tau}$ can be related to $M_{\mu\nu}^{\tau}$ in Eq. (2.9). Therefore, the additional subtraction dictated by t^{τ} for $M_{+\,\cdots\,+,\mu\nu}^{\tau}$ is determined by that for $M_{\mu\nu}^{\tau}$. The further discussion on the factorization for the decomposition shown in Fig. 6(b) follows parallel to the case for the decomposition shown in Fig. 6(a). We arrive at a formula identical to Eq. (2.20), where the v_n stands for the contributions from the bare cut vertices of two fermions and many gluons.

So far we have neglected both color and flavor degrees of freedom of quarks. Including these degrees of freedom, we find that the contributions to the moments of $\overline{W}_4^{\gamma}$ from the bare two-fermion cut vertices and the bare cut vertices for two fermions and many gluons altogether can be written in a factorized form as

$$\int_0^1 dz\, z^n \overline{W}_4^{\gamma} = v_n^{\psi} E_{4,n}^{\psi}\left[\frac{q^2}{\mu^2},g^2,\alpha\right]$$

$$+ v_n^{\mathrm{NS}} E_{4,n}^{\mathrm{NS}}\left[\frac{q^2}{\mu^2},g^2,\alpha\right] , \qquad (2.24)$$

where ψ and NS stand for flavor-singlet and -nonsinglet contributions, respectively, and μ^2 is the subtraction scale at which the theory is renormalized.

Consider now the decomposition shown in Fig. 6(c). The left-hand and right-hand parts of the graph are connected by two gluons. Let $M_{\alpha\beta,\mu\nu}^{\tau,ij}(k,q)$ be the renormalized two-gluon and two-photon amplitude. Again we write

$$M_{\alpha\beta,\mu\nu}^{\tau,ij}(k,q) = t_{\alpha\beta,\mu\nu}^{ij}(k,q) M^{\tau}(k^2,k\cdot q,q^2) , \qquad (2.25)$$

where $t_{\alpha\beta,\mu\nu}^{ij}$ is a possible tensor structure and M^{τ} is dimensionless. The appropriate tensor which contributes to $\overline{W}_4^{\gamma}$ for large q^2 and q_+ is[9]

$$t_{\alpha\beta,\mu\nu}^{ij}(k,q) = \delta_{ij}(g_{\mu\lambda}g_{\nu\kappa} - g_{\nu\lambda}g_{\mu\kappa})$$

$$\times [g^{\lambda}{}_{\alpha}g^{\kappa}{}_{\beta}k(k\cdot q)^2 - q_{\alpha}g^{\kappa}{}_{\beta}k^{\lambda}(k\cdot q) - g^{\lambda}{}_{\alpha}q_{\beta}k^{\kappa}(k\cdot q) + q_{\alpha}q_{\beta}k^{\lambda}k^{\kappa}]\frac{1}{(q^2)^2} . \qquad (2.26)$$

Multiplying $t_{\alpha\beta,\mu\nu}^{ij}$ by $\frac{1}{2}\epsilon_{-+}{}^{\mu\nu}$, we obtain for large q^2 and q_+,

$$t_{\alpha\beta,-+}^{ij}(k,q) = \frac{1}{2}\epsilon_{-+}{}^{\mu\nu} t_{\alpha\beta,\mu\nu}^{ij}(k,q)$$

$$\approx \delta_{ij}\frac{q_+^2}{(q^2)^2}[(g_{1\alpha}g_{2\beta}k_-{}^2 - g_{-\alpha}g_{2\beta}k_1 k_- - g_{1\alpha}g_{-\beta}k_2 k_-) - (\alpha\leftrightarrow\beta)] . \qquad (2.27)$$

We define the additional subtraction t^{τ} for $M_{\alpha\beta,\mu\nu}^{\tau,ij}$ as

$$t^{\tau}[\tfrac{1}{2}\epsilon_{-+}{}^{\mu\nu} M_{\alpha\beta,\mu\nu}^{\tau,ij}(k,q)] = t_{\alpha\beta,-+}^{ij}(k,q) M^{\tau}(0,\hat{k}\cdot q,q^2) . \qquad (2.28)$$

Then the contribution of Fig. 6(c) to $\overline{W}_4^{\gamma}$ is

$$\overline{W}_4^{\gamma} = \int \frac{d^4k}{(2\pi)^4}[\tfrac{1}{2}\epsilon_{-+}{}^{\rho\tau} T_{\rho\tau,\alpha\beta}^{ij}(p,k)][t^{\tau}\tfrac{1}{2}\epsilon_{-+}{}^{\mu\nu} M_{\alpha\beta,\mu\nu}^{\tau,ij}(k,q)] , \qquad (2.29)$$

where

$$T_{\rho\tau,\alpha\beta}^{ij}(p,k) = \frac{1}{2\pi}\int\int\int d^4x\, d^4y\, d^4z\, e^{ikz}e^{ip(y-x)}\langle 0|\, \overline{T}(J_{\rho}(x)A_{\alpha}^{i}(z))T(J_{\tau}(y)A_{\beta}^{j}(0))\,|0\rangle , \qquad (2.30)$$

and A_{α}^{i} is a gluon field. Using Eqs. (2.27) and (2.28), we may rewrite Eq. (2.29) as

$$\overline{W}_4^{\gamma} = \frac{q_+^2}{(q^2)^2}\int \frac{d^4k}{(2\pi)^4} T_{-+,\alpha\beta}^{ij}(p,k)\delta_{ij}[(g_{1\alpha}g_{2\beta}k_-{}^2 - g_{-\alpha}g_{2\beta}k_1 k_- - g_{1\alpha}g_{-\beta}k_2 k_-) - (\alpha\leftrightarrow\beta)]M^{\tau}(0,\hat{k}\cdot q,q^2) , \qquad (2.31)$$

where

$$T_{-+,\alpha\beta}^{ij}(p,k) = \tfrac{1}{2}\epsilon_{-+}{}^{\rho\tau} T_{\rho\tau,\alpha\beta}^{ij}(p,k) . \qquad (2.32)$$

Taking the moments of both sides of Eq. (2.31), we find

$$\int_0^1 dz\, z^n \overline{W}_4^\gamma = v_n^G E_{4,n}^G \left[\frac{q^2}{\mu^2}, g^2, \alpha \right] \,, \tag{2.33}$$

where

$$v_n^G = \tfrac{1}{8} p_-^{-n+1} \int \frac{d^4k}{(2\pi)^4} T^{ij}_{-+,\alpha\beta}(p,k)$$

$$\times 2\delta_{ij}[(g_{1\alpha}g_{2\beta}k_-^{-2} - g_{-\alpha}g_{2\beta}k_1k_- - g_{1\alpha}g_{-\beta}k_2k_-) - (\alpha \leftrightarrow \beta)]k_-^{-n-3} \,, \tag{2.34}$$

$$E_{4,n}^G \left[\frac{q^2}{\mu^2}, g^2, \alpha \right] = \int_0^1 d\tilde{z}\, \tilde{z}^{n+2} M^\tau(0, \tilde{z}, q^2) \,. \tag{2.35}$$

As in our previous discussion, we now renormalize v_n^G. The moments of $\overline{W}_4^\gamma$ are still written in the same form as Eq. (2.33). We find from Eq. (2.34) that v_n^G is the contribution from the two-gluon bare cut vertices. The form of Eq. (2.33) remains the same after we include the contributions of cut vertices with more gluons.

Finally, we examine the case where large momenta of order q^2 flow all the way down to the real-photon vertices, and the decompositions of the types shown in Fig. 6 are not adequate. Then we should consider the four-photon vertex of Fig. 7 as a whole. Call $M_{\mu\nu,\rho\tau}(p,q)$ the renormalized amplitude for the four-photon vertex, and we decompose $M_{\mu\nu,\rho\tau}(p,q)$ into the different tensor structures

$$M_{\mu\nu,\rho\tau}(p,q) = \sum_i t^i_{\mu\nu,\rho\tau}(p,q) M_i^\gamma(p^2, p\cdot q, q^2) \,. \tag{2.36}$$

We only consider the tensor which contributes to $\overline{W}_4^\gamma$ for large q^2. Then $t_{\mu\nu,\rho\tau}$ is antisymmetric in interchange of indices μ and ν or ρ and τ (we omit the superscript i of $t^i_{\mu\nu,\rho\tau}$). The appropriate one is[9]

$$t_{\mu\nu,\rho\tau}(p,q)$$
$$= \frac{1}{(q^2)^2} [(p\cdot q g_{\mu\rho} - p_\mu q_\rho)(p\cdot q g_{\nu\tau} - p_\nu q_\tau)$$
$$- (p\cdot q g_{\mu\tau} - p_\mu q_\tau)(p\cdot q g_{\nu\rho} - p_\nu q_\rho)] \,, \tag{2.37}$$

operating $\tfrac{1}{2}\epsilon_{-+}^{\mu\nu}$ on $t_{\mu\nu,\rho\tau}$, and for large q^2 and q_+ we obtain

$$\tfrac{1}{2}\epsilon_{-+}^{\mu\nu} t_{\mu\nu,\rho\tau}(p,q)$$
$$\approx \frac{q_+^2}{(q^2)^2} [(g_{1\rho}g_{2\tau}p_-^{-2} - g_{-\rho}g_{2\tau}p_1p_-$$
$$- g_{1\rho}g_{-\tau}p_2p_-) - (\rho \leftrightarrow \tau)] \,. \tag{2.38}$$

When we multiply $M_{\mu\nu,\rho\tau}(p,q)$ by $\tfrac{1}{4}\epsilon_{-+}^{\mu\nu}\epsilon_{-+}^{\rho\tau}$, we find

$$\tfrac{1}{4}\epsilon_{-+}^{\mu\nu}\epsilon_{-+}^{\rho\tau} M_{\mu\nu,\rho\tau}(p,q) \approx \frac{q_+^2 p_-^2}{(q^2)^2} M^\gamma(0,z,q^2) \,. \tag{2.39}$$

Comparing Eq. (2.39) with Eq. (2.1), we find for the contribution of graphs with the large-momentum-flow configurations shown in Fig. 7 to the photon structure function $\overline{W}_4^\gamma$,

$$\overline{W}_4^\gamma(z,q^2) = \tfrac{1}{4} z^2 M^\gamma(0,z,q^2) \,. \tag{2.40}$$

The moments are then given as

$$\int_0^1 dz\, z^n \overline{W}_4^\gamma(z,q^2) = \tfrac{1}{4} \int_0^1 dz\, z^{n+2} M^\gamma(0,z,q^2)$$
$$= E_{4,n}^\gamma \left[\frac{q^2}{\mu^2}, g^2, \alpha \right] \,. \tag{2.41}$$

The above equation can be rewritten in another form,

$$\int_0^1 dz\, z^n \overline{W}_4^\gamma(z,q^2) = v_n^\gamma E_{4,n}^\gamma \left[\frac{q^2}{\mu^2}, g^2, \alpha \right] \,, \tag{2.42}$$
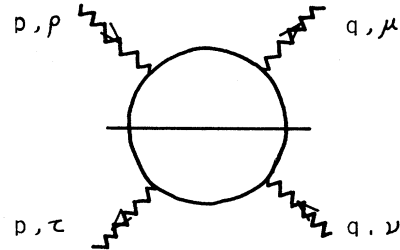
FIG. 7. The amplitude occurring in direct photon production, where large momenta of order q^2 flow through the blob.

where

$$v_n^\gamma = 1 = \tfrac{1}{2}\epsilon_- + {}^{\rho\tau}\tfrac{1}{2}p_-^{n+1}R_{\rho\tau,n}^\gamma(p) \qquad (2.43)$$

and $R_{\rho\tau,n}^\gamma(p)$ is the two-photon bare cut vertex whose expression is shown in Eq. (2.8).

Collecting all these contributions from cut vertices, i.e., Eqs. (2.24), (2.33), and (2.42), we find that the moments of $\overline{W}_4^\gamma$ are given in the following factorized form for large q^2:

$$\int_0^1 dz\, z^n\, \overline{W}_4^\gamma(z,q^2) = \sum_i v_n^i E_{4,n}^i \left[\frac{q^2}{\mu^2}, g^2, \alpha \right], \qquad (2.44)$$

where the sum i runs over ψ, G, NS, and γ. The q^2 dependence of the structure function $\overline{W}_4^\gamma$ enters into the timelike coefficient function $E_{4,n}^i$. On the other hand, v_n^i does not depend on q^2, but is dependent on the particle observed. Especially we have $v_n^\gamma = 1$ from Eq. (2.43). The hadronic feature of the observed photon is taken into account within v_n^ψ, v_n^G, and v_n^{NS}.

C. Anomalous dimensions of cut vertices

The q^2 dependence of $E_{4,n}^i$ is governed by the renormalization-group equation (RGE), which has exactly the same form as those for the case of the structure functions $\overline{W}_T^\gamma$ and $\overline{W}_L^\gamma$ in Ref. 2. The anomalous dimensions which enter into the RGE are now those of cut vertices contributing to $\overline{W}_4^\gamma$, that is, $\gamma_{4,ij}^n(g^2)$ with $i,j = \psi,G$, $\gamma_{4,\mathrm{NS}}^n(g^2)$, and $\overline{K}_{4,i}^n(g^2,\alpha)$ with $i = \psi,G,\mathrm{NS}$. They are expanded in powers of g^2 as follows:

$$\gamma_{4,ij}^n(g^2) = \gamma_{4,ij}^{0,n}\frac{g^2}{16\pi^2} + \cdots, \quad i,j = \psi,G,$$

$$\gamma_{4,\mathrm{NS}}^n(g^2) = \gamma_{4,\mathrm{NS}}^{0,n}\frac{g^2}{16\pi^2} + \cdots, \qquad (2.45)$$

$$\overline{K}_{4,i}^n(g^2,\alpha) = -\overline{K}_{4,i}^{0,n}\frac{e^2}{16\pi^2} + \cdots, \quad i = \psi,G,\mathrm{NS}.$$

The one-loop anomalous dimensions for the hadronic sector are calculated evaluating diagrams in Fig. 8. The results are

$$\gamma_{4,\psi\psi}^{0,n} = \gamma_{4,\mathrm{NS}}^{0,n} = \frac{8}{3}\left[1 - \frac{2}{n(n+1)} + 4\sum_{j=2}^n \frac{1}{j}\right],$$

$$\qquad (2.46)$$

$$\gamma_{4,\psi G}^{0,n} = -4f\frac{n+2}{n(n+1)}, \qquad (2.47)$$

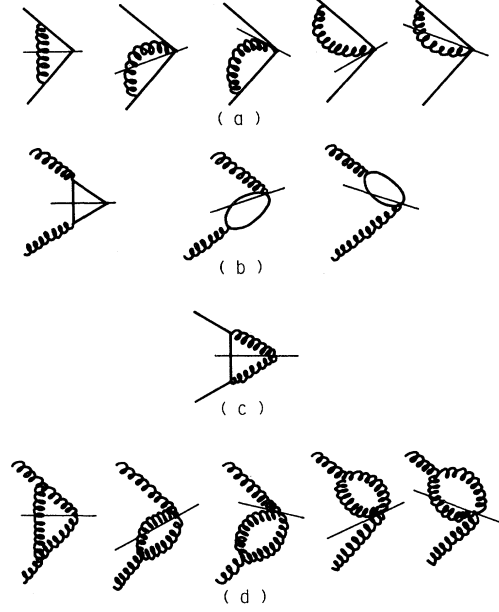FIG. 8. Diagrams for computing (a) $\gamma_{4,\psi\psi}^{0,n}$ and $\gamma_{4,\mathrm{NS}}^{0,n}$; (b) $\gamma_{4,\psi G}^{0,n}$; (c) $\gamma_{4,G\psi}^{0,n}$; (d) $\gamma_{4,GG}^{0,n}$.

$$\gamma_{4,G\psi}^{0,n} = -\frac{16}{3}\frac{n-1}{n(n+1)}, \qquad (2.48)$$

$$\gamma_{4,GG}^{0,n} = 6\left[\frac{1}{3} - \frac{8}{n(n+1)} + 4\sum_{j=2}^n \frac{1}{j}\right] + \frac{4}{3}f. \qquad (2.49)$$

The anomalous dimensions $\overline{K}_{4,\psi}^{0,n}$ and $\overline{K}_{4,\mathrm{NS}}^{0,n}$ are obtained from Eq. (2.47) by replacing the group-theory factor $f/2[=T(R)]$ by the relevant charge factors, with the result

$$\overline{K}_{4,\psi}^{0,n} = 8\frac{n+2}{n(n+1)}3f\langle e^2\rangle, \qquad (2.50)$$

$$\overline{K}_{4,\mathrm{NS}}^{0,n} = 8\frac{n+2}{n(n+1)}3f(\langle e^4\rangle - \langle e^2\rangle^2). \qquad (2.51)$$

Also we have, in the one-loop approximations,

$$\overline{K}_{4,G}^{0,n} = 0. \qquad (2.52)$$

It is interesting to compare $\gamma_{4,ij}^{0,n}$ with the anomalous dimensions $\gamma_{4,ij}^{0,n}$ which are relevant for the structure function W_4^γ in the photon-photon scatterings [see Eqs. (4.2)−(4.5) in Ref. 6]. Those $\gamma_{4,ij}^{0,n}$ also appear in the analysis of polarized electroproductions.[10] The diagonal elements are the same, i.e.,

$$\bar\gamma_{4,\psi\psi}^{0,n}=\gamma_{4,\psi\psi}^{0,n}\ ,$$

$$\bar\gamma_{4,G}^{0,n}=\gamma_{4,G}^{0,n}\ . \qquad (2.53)$$

For the off-diagonal elements we find

$$\frac{\bar\gamma_{4,\psi G}^{0,n}}{4f}=\frac{\gamma_{4,G\psi}^{0,n}}{16/3}\ ,$$

$$\frac{\bar\gamma_{4,G\psi}^{0,n}}{16/3}=\frac{\gamma_{4,\psi G}^{0,n}}{4f}\ , \qquad (2.54)$$

where $4f\,[=8T(R)]$ and $\frac{16}{3}\,[=4C_2(R)]$ are the group-theory factors.

D. Behavior of $\overline{W}_4^\gamma$

The procedures to solve the RGE now follow exactly parallel to the procedures in the case of the structure functions $\overline{W}_T^\gamma$ and $\overline{W}_L^\gamma$ or the case of the deep-inelastic scattering off the photon target.[11]

We expand the coefficient functions $E_{4,n}^i(1,\bar g^2,\alpha)$ in powers of the effective coupling constant $\bar g^2$. To the lowest order, we obtain

$$E_{4,n}^i(1,\bar g^2,\alpha)=\begin{cases}e^2\delta_\psi, & i=\psi\ ,\\ 0, & i=G\ ,\\ e^2\delta_{\rm NS}, & i={\rm NS}\ ,\end{cases} \qquad (2.55)$$

with $\delta_\psi=\langle e^2\rangle=\sum_i e_i^2/f$ and $\delta_{\rm NS}=1$.

Using this information on the lowest-order coefficient functions and one-loop anomalous dimensions, we arrive at the following formula for the moments of $\overline{W}_4^\gamma$:

$$\int_0^1 dz\, z^n \overline{W}_4^\gamma(z,q^2)=\alpha^2 \bar a_{4,n}\ln\frac{q^2}{\Lambda^2}\ , \qquad (2.56)$$

where

$$\bar a_{4,n}=\frac{1}{2}\left[\frac{\bar K_{4,\psi}^{0,n}\delta_\psi}{\bar\gamma_n}\left(1+\frac{\bar\gamma_{4,GG}^{0,n}}{2\beta_0}\right)\right.$$

$$\left.+\frac{\bar K_{4,{\rm NS}}^{0,n}\delta_{\rm NS}}{1+\bar\gamma_{4,{\rm NS}}^{0,n}/2\beta_0}\right] \qquad (2.57)$$

with

$$\bar\gamma_n=1+\frac{1}{2\beta_0}(\bar\gamma_{4,\psi\psi}^{0,n}+\bar\gamma_{4,GG}^{0,n})$$

$$+\frac{1}{4\beta_0^2}(\bar\gamma_{4,\psi\psi}^{0,n}\bar\gamma_{4,GG}^{0,n}-\gamma_{4,G\psi}^{0,n}\bar\gamma_{4,\psi G}^{0,n}) \qquad (2.58)$$

and $\beta_0=11-\frac{2}{3}f$. If we set all anomalous dimen-

sions except $\bar K_{4,\psi}^{0,n}$ and $\bar K_{4,{\rm NS}}^{0,n}$ equal to zero, we retrieve the parton-model prediction,

$$\int_0^1 dz\, z^n \overline{W}_4^\gamma\Big|_{\rm PM}=\alpha^2 \bar P_{4,n}\ln\frac{q^2}{\Lambda_{\rm PM}^2}\ , \qquad (2.59)$$

where

$$\bar P_{4,n}=4\delta_\gamma\frac{n+2}{n(n+1)}\ . \qquad (2.60)$$

The structure function $\overline{W}_4^\gamma$ itself can be obtained from the moments by taking an inverse Mellin transform. The PM formula (2.60) can be inverted analytically, and we obtain

$$\overline{W}_4^\gamma\,|_{\rm PM}=\alpha^2 P_4(z)\ln\frac{q^2}{\Lambda_{\rm PM}^2}\ , \qquad (2.61)$$

where

$$P_4(z)=4\delta_\gamma\frac{2-z}{z}\ , \qquad (2.62)$$

which coincides with the expression in Eq. (1.4). The QCD formula (2.57), on the other hand, has a complicated n dependence and has been inverted numerically.

In Fig. 9 we present both the QCD and PM predictions for $z\overline{W}_4^\gamma$ in units of $\alpha^2\ln q^2/\Lambda^2$. We find that the QCD effects are large both at small and large z values. Especially, QCD predicts that $z\overline{W}_4^\gamma$
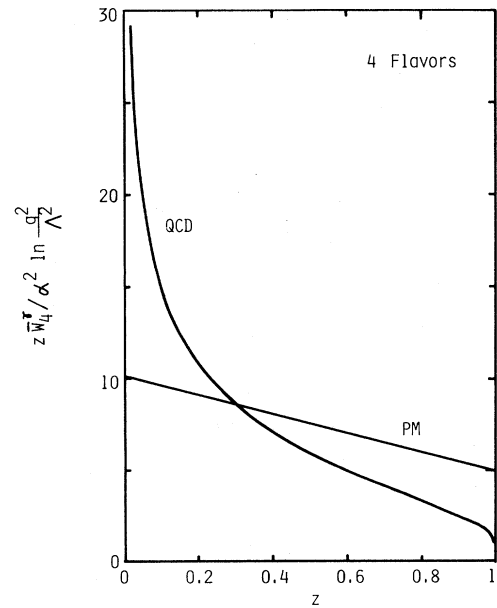
FIG. 9. The structure function $z\overline{W}_4^\gamma$ in units of $\alpha^2\ln q^2/\Lambda^2$ as predicted by (a) QCD in the leading order and (b) the parton model. We have chosen four flavors for both cases and have assumed that $\Lambda^2=\Lambda_{\rm PM}^2$.

vanishes as $-1/\ln(1-z)$ for $z\to 1$ since $\bar{a}_{4,n}$ vanishes as $1/(n\ln n)$ for large n.

III. STRUCTURE FUNCTION $\overline{W}_3^\gamma$

The moments of the structure function $\overline{W}_3^\gamma$ can also be written in a factorized form, i.e., the cut vertices times the coefficient functions. We can follow the same procedures as we did in Sec. II. Here we only show the results.

The remarkable feature of $\overline{W}_3^\gamma$ is that we cannot find the fermion cut vertices which contribute to $\overline{W}_3^\gamma$ in the leading order. Consequently, $\overline{W}_3^\gamma$ in the leading order is not renormalized by the strong interactions and agrees with the result calculated in the parton model.[12] This fact is exactly analogous to deep-inelastic scatterings off the photon target,

in which there is no twist-2 *quark* operators contributing to the structure function W_3^γ, and W_3^γ in the leading order is not affected by the strong-interaction effects and has the same expression as obtained in the parton model.[5-7]

The appropriate projection operator which picks up $\overline{W}_3^\gamma$ from $\overline{W}_{\mu\nu\rho\tau}$ in Eq. (1.2) is

$$\tfrac{1}{2}g_{1\mu}g_{2\nu}(g_{1\rho}g_{2\tau}+g_{1\tau}g_{2\rho}) ,$$

and we find for large q^2 and q_+ with finite q_- and p_μ,

$$\tfrac{1}{2}g_{1\mu}g_{2\nu}(g_{1\rho}g_{2\tau}+g_{1\tau}g_{2\rho})\overline{W}^{\mu\nu\rho\tau}\approx\overline{W}_3^\gamma . \tag{3.1}$$

The bare cut vertex for two photons contributing to $\overline{W}_3^\gamma$ has the following expression:

$$U_{\rho\tau,n}^\gamma(p)=\{[g_{1\rho}g_{2\tau}p_-^{\,2}-(g_{-\rho}g_{2\tau}p_1+g_{1\rho}g_{-\tau}p_2)p_-+g_{-\rho}g_{-\tau}p_1p_2]+[\rho\leftrightarrow\tau]\}p_-^{\,-n-3} . \tag{3.2}$$

The above form is inferred from the fact that when we multiply the specific tensor in Eq. (1.2), which projects out $\overline{W}_3^\gamma$ by $g_\mu^{\,1}g_\nu^{\,2}$, we obtain for large q_+,

$$g_1^{\,\mu}g_2^{\,\nu}\left[\left[g_{\mu\rho}-\frac{p_\mu q_\rho}{p\cdot q}\right]\left[g_{\nu\tau}-\frac{p_\nu q_\tau}{p\cdot q}\right]+\left[g_{\mu\tau}-\frac{p_\mu q_\tau}{p\cdot q}\right]\left[g_{\nu\rho}-\frac{p_\nu q_\rho}{p\cdot q}\right]\right]$$

$$\approx\frac{1}{p_-^{\,2}}\{[g_{1\rho}g_{2\tau}p_-^{\,2}-(g_{-\rho}g_{2\tau}p_1+g_{1\rho}g_{-\tau}p_2)p_-+g_{-\rho}g_{-\tau}p_1p_2]+[\rho\leftrightarrow\tau]\} . \tag{3.3}$$

The bare two-gluon cut vertices have the same form as the two-photon cut vertices except for the factor δ_{ij}:

$$U_{\rho\tau,n}^{ij}(p)=\delta_{ij}\{[g_{1\rho}g_{2\tau}p_-^{\,2}-(g_{-\rho}g_{2\tau}p_1+g_{1\rho}g_{-\tau}p_2)p_-+g_{-\rho}g_{-\tau}p_1p_2]+[\rho\leftrightarrow\tau]\}p_-^{\,-n-3} . \tag{3.4}$$

The reason why there are no fermion cut vertices contributing to $\overline{W}_3^\gamma$ in the leading order is the following. Consider again a particular decomposition of a contributing graph as shown in Fig. 6(a), where two parts are connected by two fermion propagators. Call $M_{\mu\nu}^\tau(k,q)$ the renormalized right-hand part, and we want $t^\tau M_{\mu\nu}^\tau(k,q)$ (t^τ denoting the additional subtraction operator) to be equal to the additional divergences, which arise when $q^2\to\infty$ for fixed k and fixed $k\cdot q/q^2$. Again we decompose $M_{\mu\nu}^\tau(k,q)$ into the different tensor structures as follows:

$$M_{\mu\nu}^\tau(k,q)=\sum_i t_{\mu\nu}^i(k,q)M_i^\tau(k^2,k\cdot q,q^2) , \tag{3.5}$$

where the $t_{\mu\nu}^i$ are symmetric in indices μ and ν, this time.

The candidates for contributing $t_{\mu\nu}^i$ when

$q^2\to\infty$ should be conserved tensors with no explicit factors of m^2 and k^2, and with factor k dropped compared to q. The allowed tensors are of the same form as those which have appeared in the Mueller's paper of Ref. 3:

$$t_{\mu\nu}^L=-\left[g_{\mu\nu}-\frac{q_\mu q_\nu}{q^2}\right]\frac{q}{q^2} ,$$

$$t_{\mu\nu}^2=\tfrac{1}{2}[\,2g_{\mu\nu}qq\cdot k+(\gamma_\mu k_\nu+\gamma_\nu k_\mu)q^2$$
$$-(\gamma_\mu q_\nu+\gamma_\nu q_\mu)k\cdot q$$
$$-(k_\mu q_\nu+k_\nu q_\mu)q\,]\frac{1}{(q^2)^2} . \tag{3.6}$$

Multiplying $t_{\mu\nu}^L$ and $t_{\mu\nu}^2$ by $g_1^{\,\mu}g_2^{\,\nu}$, we obtain for large q^2 and q_+,

$$g_1^{\,\mu}g_2^{\,\mu}t_{\mu\nu}^L=\frac{q_1q_2}{q^2}\frac{\gamma_-}{2q_-} , \tag{3.7}$$

$$g_1{}^\mu g_2{}^\nu t_{\mu\nu}^2 = -\tfrac{1}{2}(\gamma_1 q_2 + q_1\gamma_2)\frac{k_-}{2q_-}\frac{1}{q^2} \ .$$

Therefore, when we attach the left-hand part λ to $g_1{}^\mu g_2{}^\nu[t^\tau M_{\mu\nu}^\tau(k,q)]$, and perform the k integration and renormalization of the λ part, the resulting terms are proportional to q_1/q^2 and/or q_2/q^2. Thus the contributions from decompositions of the type shown in Fig. 6(a) to the structure function $\overline{W}_3^\gamma$ are of the order $1/q^2$ at most. In other words, there exist no fermion cut vertices which contribute to $\overline{W}_3^\gamma$.

Another support for this conclusion comes from the direct calculation of a diagram as shown in Fig. 8(c), where the bare gluon vertex $R_{\alpha\beta,n}^{ij}(k)$ of Eq. (2.4) is replaced by $U_{\rho\tau,n}^{ij}(k)$ of Eq. (3.4). If there exist fermion cut vertices contributing to $\overline{W}_3^\gamma$, then ultraviolet divergences would appear in the calculation of such diagrams. But the actual calculation gives no ultraviolet divergence.

Following the same procedures as we did in Sec. II, the moments of $\overline{W}_3^\gamma$ can be written in a factorized form

$$\int_0^1 dz\, z^n \overline{W}_3^\gamma(z,q^2) = \sum_i v_{3,n}^i E_{3,n}^i\left[\frac{q^2}{\mu^2}, g^2, \alpha\right] , \quad (3.8)$$

where the sum i runs over G and γ only, and $v_{3,n}^\gamma = 1$. The q^2 dependence of $E_{3,n}^i$ is governed by the RGE. Since there exist no fermion cut vertices and hence no mixing anomalous dimensions of order e^2, the leading term in the moments of $\overline{W}_3^\gamma$ does not grow as $\ln(q^2/\Lambda^2)$, but is constant. Solving the RGE, we obtain the QCD prediction for the moments of $\overline{W}_3^\gamma$,

$$\int_0^1 dz\, z^n \overline{W}_3^\gamma(z,q^2) = \alpha^2 \delta_\gamma \overline{B}_{3,\gamma}^n + O\left[\frac{1}{\ln q^2/\Lambda^2}\right] ,$$

$$(3.9)$$

where $\overline{B}_{3,\gamma}^n$ is the leading term which appears in the expansion of $E_{3,n}^\gamma(1,\overline{g}^2,\alpha)$, i.e.,

$$E_{3,n}^\gamma(1,\overline{g}^2,\alpha) = \frac{e^4}{16\pi^2}\delta_\gamma \overline{B}_{3,\gamma}^n + O(\overline{g}^2) . \quad (3.10)$$

Evaluating the box diagrams in Fig. 2, we obtain

$$\overline{B}_{3,\gamma}^n = -\frac{4}{n-1} \ . \quad (3.11)$$

We can easily invert the leading term of the moments of Eq. (3.9) analytically. We find that the leading term of $\overline{W}_3^\gamma$ coincides with the result (1.3) of the parton-model calculation. This fact means that $\overline{W}_3^\gamma$ in the leading order is not renormalized by the strong interactions. The origin of this in-

teresting result can be traced back to the fact that we could not construct the fermion cut vertices which give leading contributions to $\overline{W}_3^\gamma$.

IV. SUMMARY

In this paper we have analyzed in QCD the timelike photon structure functions $\overline{W}_3^\gamma$ and $\overline{W}_4^\gamma$ which can be observed in the direct-photon production in e^+e^- collisions. We have used Mueller's cut-vertex formalism and have introduced new fermion, gluon, and photon cut vertices.

The results we have obtained are very similar to the case of the spacelike photon structure functions W_3^γ and W_4^γ in the photon-photon scattering. The structure function $\overline{W}_4^\gamma$ shows the same nonscaling $\ln q^2$ behavior as predicted by the parton model, but its shape changes substantially from the PM prediction. The QCD effects are large both at small and large values of z. On the other hand, $\overline{W}_3^\gamma$ in the leading order is found not to be affected by strong interactions and to have the same expression as obtained in the parton model.

ACKNOWLEDGMENTS

APPENDIX

We present the expressions of differential cross sections for the direct-photon production

$$e^+e^- \to \gamma^*(q) \to \gamma_{\text{direct}}(p) + \text{hadrons}(C = +) \quad \text{(A1)}$$

in terms of (timelike) photon structure functions for the cases of unpolarized- and polarized-beam experiments.[1]

As shown in Fig. 1, the momenta of two incident beams are labeled by k_1 and k_2. The virtual-photon momentum is $q = k_1 + k_2$. Then, the general expression of the differential cross section for the process (A1) can be written as

$$\frac{d\sigma}{dz\,d\Omega} = \frac{3}{4\alpha q^2}\sigma_0 z \epsilon_\rho(a)\epsilon_\tau^*(a)l_{\mu\nu}\overline{W}^{\mu\nu\rho\tau}, \quad \text{(A2)}$$

where $\epsilon_\rho(a)$ is the polarization vector for the final photon with momentum p and polarization a, $z = 2v/q^2 = 2p\cdot q/q^2$, and

$$\sigma_0 = \frac{4\pi\alpha^2}{3q^2} \quad \text{(A3)}$$

is the total cross section for $e^+e^- \to \mu^+\mu^-$. $\overline{W}^{\mu\nu\rho\tau}$ is composed of photon structure functions as defined in Eq. (1.2).

In the case of the unpolarized-beam experiments, the leptonic tensor is expressed as

$$l_{\mu\nu}^U = \tfrac{1}{2}(q_\mu q_\nu - K_\mu K_\nu - q^2 g_{\mu\nu}), \quad \text{(A4)}$$

where $K = k_1 - k_2$. Since the tensor $l_{\mu\nu}^U$ is symmetric in indices μ and ν, we can obtain the information on $\overline{W}_1^\gamma$, $\overline{W}_2^\gamma$, and $\overline{W}_3^\gamma$ among four independent photon structure functions.

Let the z axis be along the incoming beam momentum $\vec{k}_1$, and the x-z plane be defined by $\vec{k}_1$ and the outgoing photon momentum $\vec{p}$. Then, two independent linear polarization vectors of the final photon are given by[13]

$$\epsilon_\rho(\perp) = \begin{bmatrix} 0 \\ 0 \\ 1 \\ 0 \end{bmatrix}, \quad \epsilon_\rho(\|) = \begin{bmatrix} 0 \\ \cos\theta \\ 0 \\ -\sin\theta \end{bmatrix}, \quad \text{(A5)}$$

where $\epsilon_\rho(\perp)$ stands for the polarization transverse to the x-z plane, and $\epsilon_\rho(\|)$ for polarization in the x-z plane. θ is the angle two vectors $\vec{k}_1$ and $\vec{p}$. Using Eqs. (A2)–(A5), and (1.2), we find that the cross section for the linear polarization of the final photon *transverse to* the plane spanned by the incident beam and the photon momentum can be written as

$$\left[\frac{d\sigma^U}{dz\,d\Omega}\right]^{(\perp)} = \frac{3}{4\alpha}\sigma_0 z\left[\overline{W}_1^\gamma + \frac{1}{2}\frac{v^2}{q^2}\sin^2\theta\,\overline{W}_2^\gamma + \tfrac{1}{2}\sin^2\theta\,\overline{W}_3^\gamma\right] \quad \text{(A6)}$$

and the cross section for the linear polarization *in* the plane is given by

$$\left[\frac{d\sigma^U}{dz\,d\Omega}\right]^{(\|)} = \frac{3}{4\alpha}\sigma_0 z\left[\overline{W}_1^\gamma + \frac{1}{2}\frac{v^2}{q^2}\sin^2\theta\,\overline{W}_2^\gamma - \tfrac{1}{2}\sin^2\theta\,\overline{W}_3^\gamma\right]. \quad \text{(A7)}$$

Therefore, the structure function $\overline{W}_3^\gamma$ is obtained by taking the difference

$$\left[\frac{d\sigma^U}{dz\,d\Omega}\right]^{(\perp)} - \left[\frac{d\sigma^U}{dz\,d\Omega}\right]^{(\|)} = \frac{3}{4\alpha}\sigma_0 z \sin^2\theta\,\overline{W}_3^\gamma. \quad \text{(A8)}$$

In order to obtain information on $\overline{W}_4^\gamma$, we must use polarized incident beams, and observe the circular polarization of the final photon. Consider the case where only the incident beam 1 is polarized with the covariant spin s_1. Then, the leptonic tensor in Eq. (A2) is written as

$$l_{\mu\nu}^P = \tfrac{1}{2}i\epsilon_{\mu\nu\alpha\beta}q^\alpha s_1^\beta. \quad \text{(A9)}$$

The tensor $l_{\mu\nu}^P$ is antisymmetric in indices μ and ν. Neglecting electron (or positron) mass m_e at high energies, we can write

$$s_1^\mu = 2\sigma_1 k_1^\mu \quad \text{(A10)}$$

with $\sigma_1 = \pm 1$, expressing the helicity state of the beam.

Then right- and left-handed circular polarization vectors are given, respectively, by

$$\epsilon_\rho(R) = \frac{1}{\sqrt{2}}\begin{bmatrix} 0 \\ \cos\theta \\ i \\ -\sin\theta \end{bmatrix}, \quad \text{(A11)}$$

$$\epsilon_\rho(L) = \frac{1}{\sqrt{2}}\begin{bmatrix} 0 \\ \cos\theta \\ -i \\ -\sin\theta \end{bmatrix}.$$

Inserting Eqs. (A9)–(A11) into (A2) and using Eq. (1.2), we obtain the following two expressions which extract the structure function $\overline{W}_4^\gamma$. (i) The difference between the cross sections for observing the final photons with the right- and left-handed circular polarizations from annihilations of polarized electrons (positrons) with helicity state σ_1 and unpolarized positrons (electrons),

$$\left[\frac{d\sigma^P}{dz\,d\Omega}\right]_R^{\sigma_1} - \left[\frac{d\sigma^P}{dz\,d\Omega}\right]_L^{\sigma_1}$$

$$= \frac{3}{4\alpha}\sigma_0 z\, 2\sigma_1\cos\theta\,\overline{W}_4^\gamma. \quad \text{(A12)}$$

(ii) The difference between the cross sections for observing the right-handed circularly polarized photon from annihilations of the unpolarized beam and the polarized beam with helicity states $\sigma_1 = +1$ and $\sigma_1 = -1$,

$$\left[\frac{d\sigma^P}{dz\,d\Omega} \right]_R^{\sigma_1=+1} - \left[\frac{d\sigma^P}{dz\,d\Omega} \right]_R^{\sigma_1=-1}$$

$$= \frac{3}{4\alpha} \sigma_0 z\, 2\cos\theta\, \overline{W}_4^\gamma \; . \qquad (A\,13)$$

---

*Operated by Universities Research Association Inc. under contract with the United States Department of Energy.

†Present address.

[1]Z. Kunszt, R. M. Muradyan, and V. M. Ter-Antonyan, Dubna Report No. E2-5347, 1970 (unpublished).

[2]K. Sasaki, Phys. Rev. D **24**, 1177 (1981).

[3]A. H. Mueller, Phys. Rev. D **18**, 3705 (1978).

[4]S. Gupta and A. H. Mueller, Phys. Rev. D **20**, 118 (1979).

[5]F. Delduc, M. Gourdin, and E. G. Oudrhiri-Safiani, Nucl. Phys. **B174**, 147 (1980); **B174**, 157 (1980).

[6]K. Sasaki, Phys. Rev. D **22**, 2143 (1980).

[7]C. Peterson, T. F. Walsh, and P. M. Zerwas, Nucl.

Phys. **B174**, 424 (1980); W. R. Frazer and G. Rossi, Phys. Rev. D **21**, 2710 (1980).

[8]We define $q_\pm = (1/\sqrt{2})(q_0 \pm q_3)$.

[9]R. Brown and I. Muzinich, Phys. Rev. D **4**, 1496 (1972).

[10]M. A. Ahmed and G. G. Ross, Phys. Lett. **B56**, 385 (1975); Nucl. Phys. **B111**, 441 (1976); H. Ito, Prog. Theor. Phys. **54**, 555 (1975); K. Sasaki, *ibid.* **54**, 1816 (1975).

[11]E. Witten, Nucl. Phys. **B120**, 189 (1977); W. A. Bardeen and A. J. Buras, Phys. Rev. D **20**, 166 (1979).

[12]This fact was first pointed out in the second paper of Ref. 5 by using the Feynman-diagram method.

[13]A four-vector x_μ is defined as $x_\mu = (t,x,y,z)$.